Supplemental Materials

Supplemental Methods

Plant material

Experiments were performed on three 8-year-old individuals of *M. glyptostroboides*, grown under glasshouse conditions for 10 weeks following a dormant overwintering period outside. Growth conditions were 16 h days, with supplemental light from sodium vapour lambs over the morning and evening providing a minimum of 300 μmol m^{-2} s^{-1} PAR at the leaf surface. Day/night temperatures were 23°C/15°C respectively. Plants were grown in 20 L pots of 8:2:1 medium of composted pine bark, course river sand and peat moss and watered daily. Once a week, plants were supplemented with liquid fertiliser (Aquasol; Hortico Ltd).

Determination of the g_s vs. Ψ_l relationship

In total, six branches were excised from the three individuals and allowed to slowly desiccate on a laboratory bench. At intervals, initially every 20-30 min but at longer intervals as branches dried out, g_s of a short shoot was measured using an infrared gas analyser (LI-6400; LI-COR Biosciences). Chamber conditions were set at a light intensity of 1000 μmol m^{-2} s^{-1} PAR (above light saturation for g_s in *M. glyptostroboides*), chamber temperature of 22°C and *D* of 1.5 kPa, the same as external conditions. Short shoots outside the chamber were illuminated with a customised fibre optic light shower. At the same time as g_s was measured, leaf water potential of an excised neighbouring short shoot was measured using a Scholander pressure chamber. The maximum duration of desiccation did not exceed 4.5 h to avoid both excessive loss of hydraulic conductivity and synthesis of ABA, the latter in *M. glyptostroboides* typically synthesised after 6 h of desiccation (McAdam and Brodribb, 2014).

Determination of the g_s vs. [ABA] relationship

The data used here for the g_s vs. [ABA] relationship in leaves of *M. glyptostroboides* is identical to that in McAdam and Brodribb (2014) and so only a brief recap of the method will be included here. Stomatal sensitivity to ABA was determined by four independent methods: (1) feeding ABA into the transpiration stream of fully hydrated, excised shoots; (2) rehydrated excised shoots previously allowed to slowly bench dry up to 24 h to stimulate ABA synthesis; (3) rehydrated excised shoots of plants undergoing drought stress; (4) *in vitro* response of stomatal aperture to ABA in solution and g_s calculated using the formula of Parlange and Waggoner (1970). In all methods bar the last one, stomatal conductance was determined by gas exchange using an infrared gas analyser. For full details of all the methods and ABA sampling, extraction, purification and quantification see McAdam and Brodribb (2014).

Shoot excision in air followed by rehydration by recutting underwater

Dynamic traces of g_s to short term changes in plant water status caused by excision in air to disrupt the hydraulic supply, followed by recutting underwater to reconnect hydraulic supply were identical to those in McAdam and Brodribb (2014), but will be described again here as the method is important for interpreting the model. Three branches were excised from the plants and after removing the periderm around the cut end of the shoots to avoid xylary blockages by resin, the branches were recut under resin-filtered deionised water. Leaves from a short shoot approximately halfway along the branch were enclosed in the chamber of an infrared gas analyser, with chamber conditions at a light intensity of 1500 μmol m^{-2} s^{-1} PAR, D of approximately 1.2 kPa and chamber temperature of 22°C. Gas exchange was automatically logged at intervals of 1 min. Leaves outside the chamber were illuminated with a customised fibre optic light shower, providing a minimum of 300 μmol m^{-2} s^{-1} PAR at the leaf surface. Once a steady-state was reached (defined as less than 3% change in g_s over 8 min), the cut end of the branch was removed from the water and excess water around the cut dried with paper towel to remove hydraulic supply to the branch. The branch was allowed to dehydrate and stomata close to approximately 50% of the initial g_s, at which point the branch was rehydrated by recutting the branch underwater to reconnect hydraulic supply. Samples for ABA quantification were taken at the initial steady-state, at the minimum g_s and at the final steady-state following rehydration on neighbouring short shoots.

Rehydration following drought

An individual plant was droughted by withholding water and branches sampled at 6, 10, 14 and 21 days post cessation of watering. Leaves from a short shoot were enclosed in an infrared gas analyser chamber with chamber conditions at a light intensity of 1000 μmol m^{-2} s^{-1} PAR, D of approximately 1.2 kPa and chamber temperature of 22°C. Chamber conditions and gas exchange were automatically logged at intervals of 1 min. Prior to rehydration, a tissue sample from a neighbouring short shoot was taken for ABA quantification. The branch was rehydrated by recutting the branch underwater in resin-filtered deionised water to reconnect hydraulic supply instantaneously. ABA extraction, purification and quantification were as described in McAdam and Brodribb (2014).

Model fitting and data analysis

Values for hydraulic parameters K and C used in the model were the mean values obtained by Martins et al. (2016), except for the rehydration kinetic after 21 days drought, where the leaf water potential was sufficiently low for significant hydraulic loss to have occurred (Table 1). In this case, K was calculated from the vulnerability curve in McAdam and Brodribb (2014). Values for stomatal conductance sensitivity to turgor pressure χ were estimated from the linear region of g_s vs. Ψ_l relationships from excised leaves (slope of the relationship should be χ; Supplemental Fig. S1; Table 1). These values were then used to fit eqn 8 to g_s vs. [ABA] data (Fig. 1), allowing M, d and $[ABA]_0$ to be fitted to minimise sum of squares. All parameters were used unaltered to calculate dynamic solutions for the cases of excision-rehydration (eqn 12a during dehydration, eqn 12b following rehydration) and rehydration following drought using the ABA concentrations obtained from experiment (eqn 13). In modelling the response to rehydration following drought, reconnection of hydraulic supply was taken to occur at time $t = 0$ s.

Fitting the Hill equation variant of ABA dependence (eqn S19) to g_s vs. [ABA] data used K, C and χ as above and allowed d, M, K_A, k_3/k_1 and n to be unconstrained while minimising the sum of squares. Fitting of the Tardieu and Davies model to g_s vs. [ABA] data required more constraints. As the Tardieu and Davies model (eqn S20) requires both [ABA] and Ψ_l, an effective Ψ_l was reconstructed from the g_s vs. [ABA] data using the known values of g_s, D and P_{atm} and the mean value for K using eqn S26. Initially g_{min}, α, β and δ were allowed to be fitted to minimise sum of squares; however, the best fit produced $\delta > 0$, resulting in wrong-

way dynamics to changes in Ψ_l. Fitted g_{min} also tended to be higher than g_s observed in some of the drier rehydration kinetics. Instead, g_{min} was set at 0.005 mol m^{-2} s^{-1} and the Tardieu and Davies model fitted to the steady state g_s vs. [ABA] for different values of δ. Simulations with these parameters using eqns S20, S24, S25 and S26 were then compared with the observed excision-rehydration kinetics until a good fit was obtained. Once a good parameter set was obtained, this set was used to simulate rehydration kinetics using eqns S20, S24, S25 and S27.

The observed rehydration kinetics were compared with exponential dynamics by fitting exponential curves of the form $g_s = A + B\exp(-t/\tau)$, fitting by minimising the sum of squares. Fitted steady state g_s was obtained as the parameter A, while the fitted halftime was calculated from τ as $t_{1/2} = \tau ln2$. Bounds were placed on the expected range of halftimes by selecting the minimum and maximum values for C/K observed within branches and using the corresponding C in those branches, while χ and D were kept constant. Values for C and K in these cases were: 797.2 mmol m^{-2} MPa^{-1} and 3.61 mmol m^{-2} s^{-1} MPa^{-1} respectively for the minimum case; 1525 mmol m^{-2} MPa^{-1} and 4.51 mmol m^{-2} s^{-1} MPa^{-1} respectively for the maximum case. Note that these do not correspond to the extremum of C and K. Halftime bounds were then calculated using eqn 9. Steady state g_s obtained by fitting the exponential curves was compared with the modelled steady state g_s using average plant parameters by performing a two-tailed paired t-test on the residuals to see whether the mean was significantly different from 0. The expected range in steady state g_s was modelled using the observed range in K and eqn 8. Maximum observed K was 4.51 mmol m^{-2} s^{-1} MPa^{-1}, while minimum observed was 2.47 mmol m^{-2} s^{-1} MPa^{-1}.

Supplemental Model Development

The ABA hydraulic model

A full derivation of the ABA hydraulic model is provided here. As mentioned in the text, the hydraulic core of the model at the leaf level was based on inward and outward fluxes of water, following Jones (1982):

$$\frac{dW}{dt} = J - E \qquad \text{eqn 1}$$

where W is the water content of the leaf per leaf area (mol m^{-2}), t is time (s), J is the flux of liquid water entering the leaf (mol m^{-2} s^{-1}) and E is the flux of water vapour lost from the leaf by transpiration (mol m^{-2} s^{-1}).

Using an Ohm's Law approximation, the flux of water into the leaf can be expressed as

$$J = K(\Psi_s - \Psi_l) \qquad \text{eqn S1}$$

where K is the hydraulic conductivity of the leaf (mol m^{-2} s^{-1} Pa^{-1}), Ψ_s is the source water potential and Ψ_l is the leaf water potential (both in units of Pa).

Assuming well-mixed conditions, i.e. a negligible boundary layer resistance, the flux of water out of the leaf can be expressed as

$$E = \frac{g_s D}{P_{atm}} \qquad \text{eqn S2}$$

where g_s is stomatal conductance (mol m^{-2} s^{-1}), D is the vapour pressure difference (Pa) and P_{atm} is atmospheric pressure (Pa).

By definition of capacitance as the change in leaf water content per change in leaf water potential and the chain rule, the rate of change of water content can be expressed in terms of water potential as

$$\frac{dW}{dt} = \frac{dW}{d\Psi_l}\frac{d\Psi_l}{dt} = C\frac{d\Psi_l}{dt} \qquad \text{eqn S3}$$

Combining eqns 1, S1, S2 and S3 and diving through by C, eqn 2 is obtained:

$$\frac{d\Psi_l}{dt} = \frac{K}{C}(\Psi_s - \Psi_l) - \frac{g_s D}{C P_{atm}} \qquad \text{eqn 2}$$

A more in depth expression for g_s is now required. In general, stomatal pore area and by extension stomatal conductance is a function of both guard cell and epidermal turgor pressures (Franks et al., 1998; Franks and Farquhar, 2007), with guard cell turgor (P_g) acting to open stomata while epidermal turgor pressure acting to reduce pore aperture. In angiosperms the control of stomatal aperture can be dominated by the epidermis and is

known as mechanical advantage, occasionally leading to transient wrong way responses of stomata to changes in plant water status (Franks et al., 1998; Buckley et al., 2003; Buckley, 2005). No mechanical advantage or wrong-way response has been observed in ferns (Franks and Farquhar, 2007; Brodribb and McAdam, 2011), while conifers appear to also exhibit no wrong-way response (McAdam and Brodribb, 2012; McAdam and Brodribb, 2014; Martins et al., 2016). It has been suggested the reduced influence of epidermal turgor on stomatal aperture in ferns, lycophytes and gymnosperms is due to greater lignification of the dorsal walls of guard cells in these lineages compared with angiosperms (McAdam and Brodribb, 2014). Ignoring the influence of the epidermis, stomatal conductance was assumed to be a linear function of P_g (Cowan, 1972; Dewar, 1995; 2002; Buckley et al., 2003; Buckley, 2005)

$$g_s = \chi\left(P_g - P_0\right) \quad \text{eqn 3}$$

where P_0 is the guard cell turgor pressure where stomata fully close and χ is the constant of proportionality.

Expressing P_g as

$$P_g = \Psi_g + \pi_g \quad \text{eqn S4}$$

where Ψ_g and π_g are guard cell water potential and osmotic pressure respectively, eqn 3 can be expressed in terms of water potential as

$$g_s = \chi\left(\Psi_g + \pi_g - P_0\right) \quad \text{eqn S5}$$

A treatment of guard cell water relations is now required. Although it has been suggested the guard cell hydraulic connection with the rest of the plant occurs via the vapour phase (Peak and Mott, 2011), a liquid phase hydraulic connection was favoured in the model. Meidner (1975) suggested a major proportion of total evaporative loss of water into the atmosphere occurred through the guard cells, a process known as peristomatal transpiration. This assumption has been used in the models of Dewar (1995; 2002), while Buckley et al. (2003) allowed for the division of evaporation between the epidermis and guard cells. Provided some transpiration occurs directly from guard cells, a water potential gradient will occur between the guard cells and the rest of the leaf. However, guard cells possess thick cuticles on the exterior surface and in the throat of the pore, and it would appear unfavourable for the plant to be losing most of its water through peristomatal transpiration. It was therefore assumed that most evaporation occurred within the mesophyll. Moreover, it was assumed there was

178 negligible hydraulic resistance between the rest of the leaf and the guard cells. Both
179 assumptions are consistent with a previous iterative hydraulic model that successfully
180 predicted dynamics to changes in water status in ferns and conifers (Brodribb and McAdam,
181 2011; McAdam and Brodribb, 2014; Martins et al., 2016). The assumptions of a negligible
182 resistance between the guard cell and the rest of the leaf and negligible transpiration
183 occurring directly from the guard cells leads to

184 $$\Psi_g = \Psi_l \qquad \text{eqn S6}$$

185 In the light, the guard cell turgor pressure is higher than the turgor pressure of the epidermis
186 and mesophyll cells due to the active accumulation of solutes in the guard cells, such as
187 potassium and malate (Kollist et al., 2014). In the model, the osmotic pressure in the guard
188 cells was assumed to be composed of two components: the first consisted of the background
189 osmotic pressure of the leaf and was assumed unaffected by active processes (π_l); the second
190 consisted of a component that could be actively regulated by metabolic processes in the guard
191 cell, such as light-induced build up of osmolytes or the ABA-induced efflux of solutes (π_a). It
192 was also assumed changes in volume of the guard cell are small so that the osmotic pressure
193 of the guard cell do not change appreciably with changes in volume. This last assumption is
194 probably violated in angiosperms as guard cell volume can greatly change between closed
195 and fully open states (Raschke, 1975), although volume change is expected to be smaller in
196 conifers due to larger guard cell size.

197 Equation S5 then becomes

198 $$g_s = \chi(\Psi_l + \pi_a + \pi_l - P_0) \qquad \text{eqn S7}$$

199 and letting $d = \pi_l - P_0$ gives eqn 4.

200 The active metabolic control of stomatal conductance occurs through π_a, while hydropassive
201 control occurs through Ψ_l. In general, a description of inward and outward fluxes of
202 osmolytes in terms of ion channel behaviour is difficult (Hills et al., 2012), while the role of
203 osmolyte synthesis in the guard cells is still unclear (Lawson, 2009). Instead, simple
204 expressions were used to describe the inward flux or accumulation of osmolytes in the guard
205 cells in the light, and the outward flux of osmolytes triggered by ABA. Although both inward
206 and outward fluxes of solutes are often driven by changes in guard cell membrane potential
207 (Hills et al., 2012), here it was assumed both processes occurred independently. However, it
208 will be shown that this assumption can be identical mathematically to a case where the light

driven influx of solutes is reduced by the presence of ABA, as expected for depolarisation of the membrane.

The flux of solutes into the guard cell was assumed to be proportional to the difference between the current osmotic pressure and a target osmotic pressure (*M*) obtainable in the absence of ABA, set by environmental conditions such as light, temperature and carbon dioxide concentration (Kirschbaum et al., 1988; Haefner et al., 1997):

$$inward\ flux = k_1(M - \pi_a) \qquad \text{eqn S8}$$

where k_1 is the rate constant for the inward flux.

The flux of solutes out of the guard cell was assumed to be dependent on the level of ABA within the leaf ([ABA]) and π_a by simple mass action. This assumption is analogous to the activation of outward channels being proportional to [ABA] and the resulting loss of solutes occurring by simple collision kinetics. Although in practice efflux kinetics would be much more complex, the simplest case was used as a first approximation. This gave

$$outward\ flux = k_2\pi_a[\mathrm{ABA}] \qquad \text{eqn S9}$$

where k_2 is the rate constant for the outward flux.

The equation for osmotic pressure of the guard cell becomes

$$\frac{d\pi_a}{dt} = k_1(M - \pi_a) - k_2\pi_a[\mathrm{ABA}] \qquad \text{eqn S10}$$

As mentioned earlier, it could be argued that ABA reduces the osmotic pressure of the guard cell through either reducing the maximum osmotic pressure obtainable, equivalent to depolarising the membrane, or through activating efflux channels, or a combination of both. However, upon rearranging eqn S10,

$$\frac{d\pi_a}{dt} = (k_1 + k_2[\mathrm{ABA}])\left(\frac{k_1}{k_1 + k_2[\mathrm{ABA}]}M - \pi_a\right) \qquad \text{eqn S11}$$

This is equivalent to ABA reducing the maximum possible osmotic pressure for the guard cell, while also increasing the rate at which equilibrium is achieved. Thus the two interpretations are effectively equivalent.

In testing the model, inward and outward fluxes and thus the net flux balance was considered constant for the short-term dynamics in plant water status. At steady state the flux balance gives

$$k_1(M - \pi_a) = k_2\pi_a[\mathrm{ABA}] \qquad \text{eqn 5}$$

which upon rearrangement gives

$$\pi_a = \frac{M}{1+\frac{[\mathrm{ABA}]}{[\mathrm{ABA}]_0}} \qquad \text{eqn 6}$$

where $[\mathrm{ABA}]_0$ is the ratio of inward and outward rate constants and is the [ABA] where π_a is half the maximum value.

The goal now is to express eqn 2 in terms of g_s. Expressing eqn 4 in terms of Ψ_l and substituting into eqn 2, noting that π_a is constant over the short-term dynamics in plant water status gives

$$\frac{dg_s}{dt} = \frac{\chi K}{C}\left(\frac{M}{1+\frac{[\mathrm{ABA}]}{[\mathrm{ABA}]_0}} + \Psi_s + d\right) - \frac{1}{C}\left(K + \frac{\chi D}{P_{atm}}\right) g_s \qquad \text{eqn 7}$$

Steady-state g_s is obtained by letting $\frac{dg_s}{dt} = 0$. For a plant with hydraulic supply connected, this gives

$$g_s^* = \frac{\chi}{1+\frac{\chi D}{KP_{atm}}}\left[\frac{M}{1+\frac{[\mathrm{ABA}]}{[\mathrm{ABA}]_0}} + \Psi_s + d\right] \qquad \text{eqn 8}$$

For the case of where hydraulic supply is not connected, such as when a leaf is excised in air, $K = 0$ and by inspection of eqn 7 gives a steady state of $g_s^* = 0$.

For constant plant parameters, eqn 7 is a linear ordinary differential equation for g_s and gives exponentials as analytical solutions

$$g_s = g_1 e^{-\frac{t}{C}\left(K+\frac{\chi D}{P_{atm}}\right)} + g_s^* \qquad \text{eqn S12}$$

where g_1 is a constant with units of conductance, dependent on initial conditions.

From eqn S12, it can be seen that the halftime for a dynamic is dependent on two component halftimes characteristic of hydraulic and evaporative processes respectively. The total halftime

$$t_{1/2\ total} = \frac{C\ ln\ 2}{\left(K + \frac{\chi D}{P_{atm}}\right)} \quad \text{eqn 9}$$

is the halftime for a step change in hydraulic supply or demand where the plant is both hydraulically connected and transpiring. If the leaf is not transpiring ($D = 0$), such as in the rehydration method for determining K and C (Blackman and Brodribb, 2011), the halftime becomes

$$t_{1/2\ hydraulic} = \frac{C}{K} ln\ 2 \quad \text{eqn 10}$$

and is denoted here as the hydraulic halftime as it depends only on the hydraulic properties of the leaf.

If the leaf is transpiring but has no hydraulic supply ($K = 0$), the halftime becomes

$$t_{1/2\ evaporative} = \frac{CP_{atm}}{\chi D} ln\ 2 \quad \text{eqn 11}$$

and is denoted here as the evaporative halftime as it depends on the evaporative properties of the leaf. The total halftime can thus be represented as

$$t_{1/2\ total} = \frac{1}{\left(\frac{1}{t_{1/2\ hydraulic}} + \frac{1}{t_{1/2\ evaporative}}\right)} \quad \text{eqn S13}$$

From eqn S13 it can be seen that the total halftime will be less than the two component halftimes.

The model was tested under two scenarios. In the first, a fully hydrated branch was excised in air, cutting off hydraulic supply. As the leaves dried out, stomata closed, before the branch was recut underwater to reconnect hydraulic supply. If the initial excision occurred at $t = 0$, then $K = 0$ up until recutting underwater at $t = t_r$. For $t < t_r$, eqn S12 becomes

$$g_s = g_s^* e^{-\left(\frac{\chi D}{CP_{atm}}\right)t} \quad \text{eqn 12a}$$

For $t > t_r$, the full form of eqn S12 applies. Matching the boundary condition at $t = t_r$ gives

$$g_1 = g_s^* \left(e^{\frac{K}{C}t_r} - e^{\left(\frac{K}{C} + \frac{\chi D}{CP_{atm}}\right)t_r}\right) = -g_s^* e^{\frac{t_r}{C}\left(K + \frac{\chi D}{P_{atm}}\right)} \left(1 - e^{-\left(\frac{\chi D}{CP_{atm}}\right)t_r}\right) \quad \text{eqn S14}$$

Substituting into eqn S12 gives, for $t > t_r$

$$g_s(t) = g_s^* \left\{ 1 - \left[1 - e^{-\left(\frac{\chi D}{CP_{atm}}\right)t_r} \right] e^{-\left(\frac{K}{C} + \frac{\chi D}{CP_{atm}}\right)(t - t_r)} \right\} \quad \text{eqn 12b}$$

In the second scenario, branches of droughted plants were rehydrated by excision underwater. If the initial g_s was g_{s0} and cutting underwater occurred at $t = 0$, then

$$g_1 = g_{s0} - g_s^* \quad \text{eqn S15}$$

Substituting into eqn S12 then gives

$$g_s(t) = (g_{s0} - g_s^*) e^{-\left(\frac{K}{C} + \frac{\chi D}{CP_{atm}}\right)t} + g_s^* \quad \text{eqn 13}$$

Hill equation kinetics variant for ABA sensitivity

To compare the form used above for g_s sensitivity to ABA against other similar alternative forms, the steady state model was modified to use a general Hill equation form for ABA-driven efflux of solutes from the guard cell. In this scenario, the activation of ion channels was seen to follow Hill equation kinetics, while the loss of solutes still followed simple mass action. Influx of solutes into the guard cell was kept unchanged from the original model. Using Hill equation kinetics, the outward flux of solutes can be represented as

$$outward\ flux = \frac{k_3 \pi_a}{\left(\frac{K_A}{[\mathrm{ABA}]}\right)^n + 1} \quad \text{eqn S16}$$

where k_3 is the rate constant for efflux, K_A is the level of ABA where half the channels are active and n is the Hill coefficient. Combining with eqn S8, the equation for balance of inward and outward fluxes of solutes becomes

$$k_1(M - \pi_a) = \frac{k_3 \pi_a}{\left(\frac{K_A}{[\mathrm{ABA}]}\right)^n + 1} \quad \text{eqn S17}$$

Rearranging, eqn S17 becomes

$$\pi_a = \frac{M}{1 + \frac{k_3/k_1}{\left(\frac{K_A}{[\mathrm{ABA}]}\right)^n + 1}} \quad \text{eqn S18}$$

Equation S18 was then substituted in place of the ABA dependence of eqn 8 to yield

$$g_s^* = \frac{\chi}{1+\frac{\chi D}{KP_{atm}}}\left[\frac{M}{1+\frac{k_3/k_1}{\left(\frac{K_A}{[\mathrm{ABA}]}\right)^n+1}} + \Psi_s + d\right] \quad \text{eqn S19}$$

Tardieu and Davies model

For a comparison of the model with the currently used model for ABA dependence of g_s, the model of Tardieu and Davies (1993) was modified to fit with the experimental test conditions. The model of Tardieu and Davies uses an empirical form to relate [ABA] and Ψ_l to g_s:

$$g_s = g_{min} + \alpha exp\left(\beta[\mathrm{ABA}]exp(\delta\Psi_l)\right) \quad \text{eqn S20}$$

where g_{min} is the minimum value for g_s, α is the maximum difference from g_{smin} in the absence of ABA, β is the sensitivity to [ABA] and δ is the sensitivity to leaf water potential. Whereas the original model of Tardieu and Davies took [ABA] to be the concentration of ABA in the xylem sap, here it was taken to be the level of ABA in the leaf.

The original formulation of the Tardieu and Davies model (Tardieu and Davies, 1993) was aimed at steady-state or a quasi-steady state condition. The level of ABA was a flux balance of ABA coming into the leaf from the xylem sap, ABA lost through the transpiration stream and ABA catabolised:

$$[\mathrm{ABA}] = \frac{J_{ABA}}{J+b} \quad \text{eqn S21}$$

where J_{ABA} is the flux of ABA synthesised in the roots, J (= E at steady state) is the flux of water through the leaf and b is the flux catabolised.

The Tardieu and Davies model was modified to be applicable to the short-term changes in plant water relations used to test the hydraulic ABA model. The modified model still described the [ABA] in the leaf as a result of a flux balance of ABA transported into the leaf by the liquid flux and the loss of ABA through transpiration, but in the non-steady state the fluxes were not equal. For short-term changes in plant water relations, changes in plant water status were of too short a duration to significantly affect ABA biosynthesis or catabolism, thus the rate of catabolism was set to zero. Moreover, as biosynthesis was assumed to be

negligible over a similar timeframe, the [ABA] in the xylem sap was assumed to be the same as the bulk leaf tissue. The rate of change of [ABA] in the leaf was given by

$$\frac{d[ABA]}{dt} = \frac{18}{FWA}\left(J[ABA]_x - E[ABA]\right) \qquad \text{eqn S22}$$

where $[ABA]_x$ is the level of ABA in the xylem sap and FWA is the fresh weight of leaves per unit area (g m^{-2}). The factor 18 (g mol^{-1}) is to convert the molar water fluxes into mass fluxes.

Modelling plant water relations for the Tardieu and Davies model began at eqn 2. As g_s in the Tardieu and Davies model is no longer a linear function of Ψ_l, a numerical solution is required. Crudely discretising eqn 2 and letting $\Psi_s = 0$ as was the case for the model tests leads to

$$\frac{\Psi_{l\,t+1} - \Psi_{l\,t}}{\Delta t} = \frac{1}{C}\left(-K\Psi_{l\,t} - \frac{g_s([\mathrm{ABA}],\Psi_{l\,t})D}{P_{atm}}\right) \qquad \text{eqn S23}$$

where $\Psi_{l\,t+1}$ and $\Psi_{l\,t}$ are the next and current values of Ψ_l respectively, Δt is the time step between calculations and g_s has the Tardieu and Davies form (eqn S20) and is evaluated at $\Psi_{l\,t}$. Rearranging gives the iterative solution for Ψ_l as

$$\Psi_{l\,t+1} = \Psi_t + \frac{\Delta t}{C}\left(-K\Psi_{l\,t} - \frac{g_s([\mathrm{ABA}],\Psi_{l\,t})D}{P_{atm}}\right) \qquad \text{eqn S24}$$

Discretising eqn S22 leads to

$$[\mathrm{ABA}]_{t+1} = \frac{18\Delta t}{FWA}J[\mathrm{ABA}]_x - \left(\frac{18\Delta t}{FWA}E - 1\right)[\mathrm{ABA}]_t \qquad \text{eqn S25}$$

where J and E were calculated using eqn S1 and S2.

Initial steady-state Ψ_l for excision-rehydration kinetics was calculated by iteration using eqn S20 and

$$\Psi_l = \frac{-g_s D}{KP_{atm}} \qquad \text{eqn S26}$$

Initial Ψ_l for rehydration kinetics were calculated by inverting eqn S20:

$$\Psi_l = \frac{1}{\delta} ln\left(\frac{1}{\beta[\mathrm{ABA}]}\ln\left(\frac{g_s - g_{min}}{\alpha}\right)\right) \qquad \text{eqn S27}$$

At the start of both excision-rehydration and rehydration kinetics, $[ABA]_x$ and [ABA] were assumed to be in equilibrium.

Combining eqn S24, S25, the relevant initial condition and evaluating g_s using eqn S20 at each time step produced the modelled dynamics for the Tardieu and Davies model, noting that during dehydration kinetics hydraulic supply was disconnected, i.e. $K = 0$.

Literature Cited

Blackman CJ, Brodribb TJ (2011) Two measures of leaf capacitance: insights into the water transport pathway and hydraulic conductance in leaves. Functional Plant Biology 38: 118-126

Brodribb TJ, McAdam SAM (2011) Passive origins of stomatal control in vascular plants. Science 331: 582-585

Buckley TN (2005) The control of stomata by water balance. New Phytologist 168: 275-291

Buckley TN, Mott KA, Farquhar GD (2003) A hydromechanical and biochemical model of stomatal conductance. Plant, Cell and Environment 26: 1767-1785

Christmann A, Weiler EW, Steudle E, Grill E (2007) A hydraulic signal in root-to-shoot signalling of water shortage. The Plant Journal 52: 167-174

Cowan IR (1972) Oscillations in stomatal conductance and plant functioning associated with stomatal conductance: observations and a model. Planta 106: 185-219

Dewar RC (1995) Interpretation of an empirical model for stomatal conductance in terms of guard cell function. Plant, Cell and Environment 18: 365-372

Dewar RC (2002) The Ball-Berry-Leuning and Tardieu-Davies stomatal models: synthesis and extension within a spatially aggregated picture of guard cell function. Plant, Cell and Environment 25: 1383-1398

Franks PJ, Cowan IR, Farquhar GD (1998) A study of stomatal mechanics using the cell pressure probe. Plant, Cell and Environment 21: 94-100

Franks PJ, Farquhar GD (2007) The mechanical diversity of stomata and its significance in gas-exchange control. Plant Physiology 143: 78-87

Haefner JW, Buckley TN, Mott KA (1997) A spatially explicit model of patchy stomatal responses to humidity. Plant, Cell and Environment 20: 1087-1097

Hills A, Chen ZH, Amtmann A, Blatt MR, Lew VL (2012) OnGuard, a computational platform for quantitative kinetic modeling of guard cell physiology. Plant Physiology 159: 1026-1042

Jones HG (1982) 'Plants and microclimate'. Cambridge University Press, Cambridge, UK

Kirschbaum MUF, Gross LJ, Pearcy RW (1988) Observed and modeled stomatal responses to dynamic light environments in the shade plant Alocasia macrorrhiza. Plant, Cell and Environment 11: 111-121

Kollist H, Nuhkat M, Roelfsema MRG (2014) Closing gaps: linking elements that control stomatal movement. New Phytologist 203: 44-62

Lawson T (2009) Guard cell photosynthesis and stomatal function. New Phytologist 181: 13-34

Martins SCV, McAdam SAM, Deans RM, DaMatta FM, Brodribb TJ (2016) Stomatal dynamics are limited by leaf hydraulics in ferns and conifers: results from simultaneous measurements of liquid and vapour fluxes in leaves. Plant, Cell and Environment 39: 694-705

McAdam SAM, Brodribb TJ (2012) Fern and lycophyte guard cells do not respond to endogenous abscisic acid. Plant Cell 24: 1510-1521

McAdam SAM, Brodribb TJ (2014) Separating active and passive influences on stomatal control of transpiration. Plant Physiology 164: 1578-1586

Meidner H (1975) Water supply, evaporation, and vapour diffusion in leaves. Journal of Experimental Botany 26: 666-672

Peak D, Mott KA (2011) A new, vapour-phase mechanism for stomatal responses to humidity and temperature. Plant Cell and Environment 34: 162-178

Raschke K (1975) Stomatal action. Annual Review of Plant Physiology 26: 309-340

Tardieu F, Davies WJ (1993) Integration of hydraulic and chemical signalling in the control of stomatal conductance and water status of droughted plants. Plant, Cell and Environment 16: 341-349

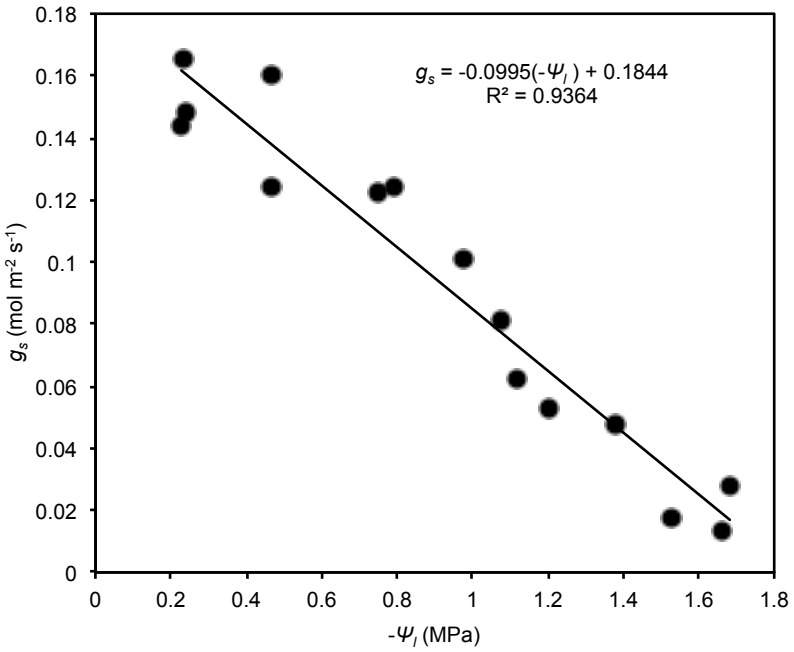

411

412 **Supplemental Figure S1.** The linear range of dependence of stomatal conductance on leaf water
413 potential for *M. glyptostroboides*. χ was estimated as the slope of the linear line of best fit for stomatal
414 conductance vs. leaf water potential. Within this range of water potentials, the assumption that
415 stomatal conductance was a linear function of turgor pressure appeared valid.

416

417

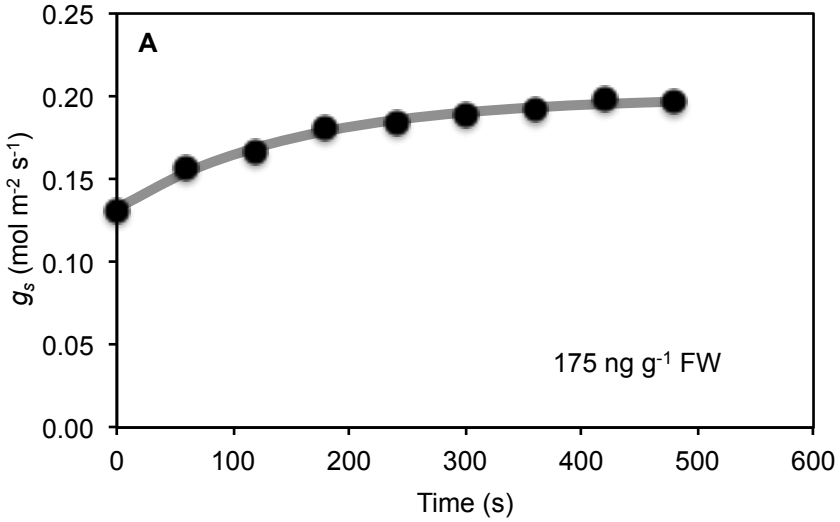

418

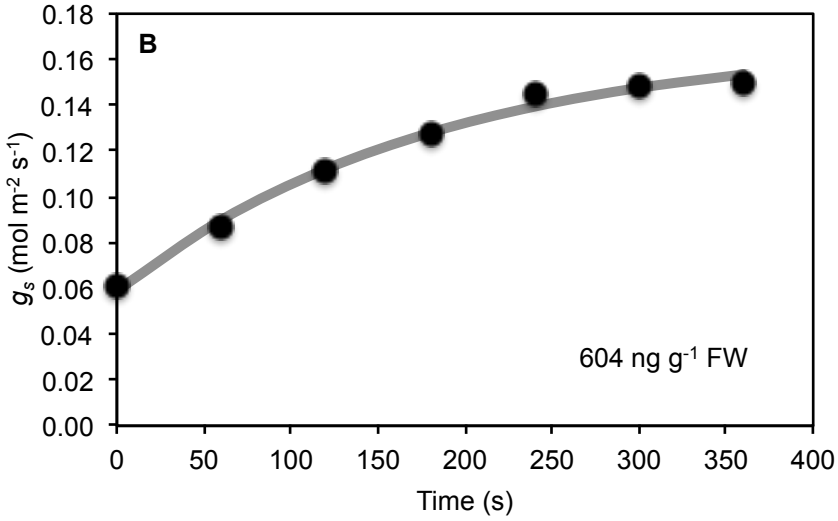
B
604 ng g-1 FW
gs (mol m-2 s-1)
Time (s)
0.18
0.16
0.14
0.12
0.10
0.08
0.06
0.04
0.02
0.00
0
50
100
150
200
250
300
350
400

419

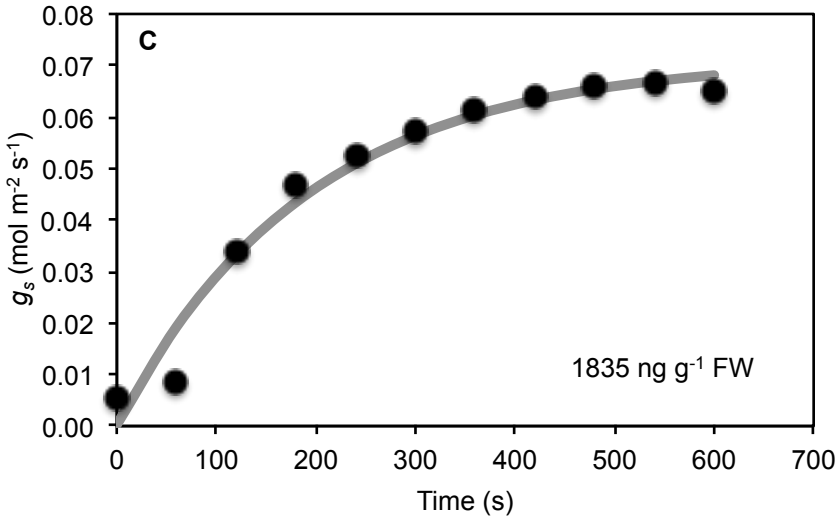
C
1835 ng g-1 FW
gs (mol m-2 s-1)
Time (s)
0.08
0.07
0.06
0.05
0.04
0.03
0.02
0.01
0.00
0
100
200
300
400
500
600
700

420

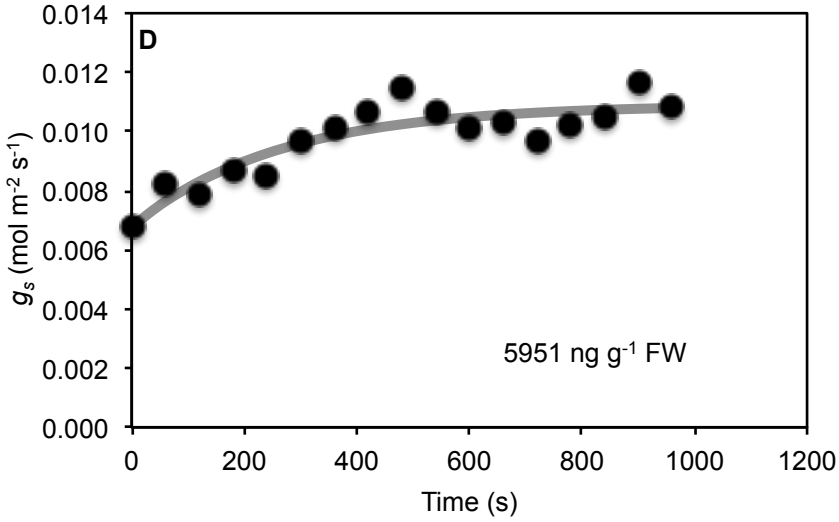
D
5951 ng g-1 FW
gs (mol m-2 s-1)
Time (s)
0.014
0.012
0.010
0.008
0.006
0.004
0.002
0.000
0
200
400
600
800
1000
1200

421

Supplemental Figure S2. Exponential fits to observed kinetics of stomatal conductance recovery upon recutting underwater, following drought to increase leaf ABA levels. Exponentials fitted the observed kinetics well at most ABA levels (A, 175 ng g^{-1}, R^2 = 0.99; B, 604 ng g^{-1}, R^2 = 0.99; C, 1835 ng g^{-1}, R^2 = 0.97; A, 5951 ng g^{-1}, R^2 = 0.81).

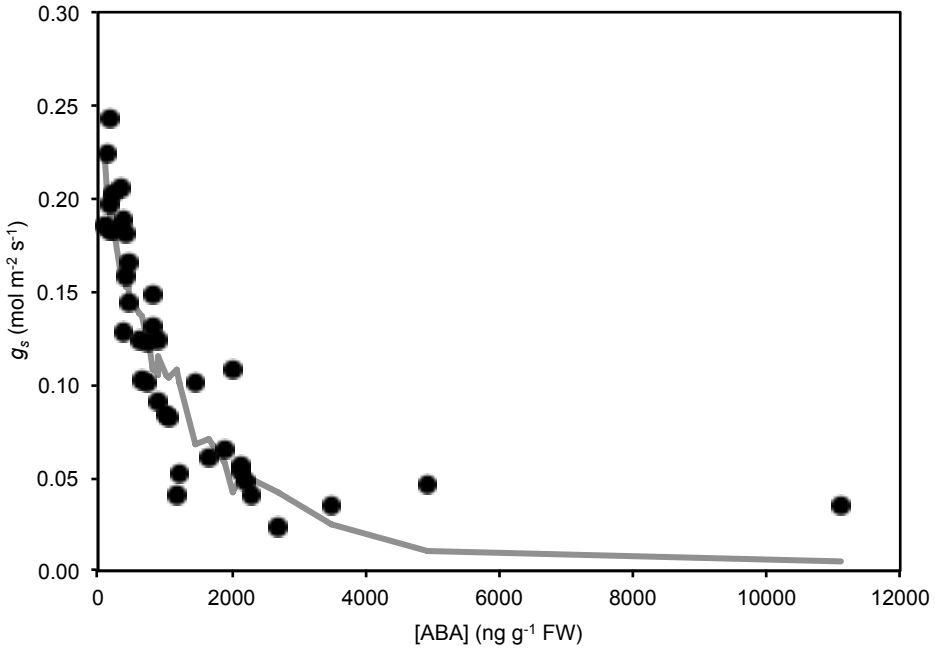

Supplemental Figure S3. Tardieu and Davies model (eqn S20) fitted to data from McAdam and Brodribb (2014), showing the dependence of fully hydrated stomatal conductance on leaf ABA levels (R^2 = 0.80). A stomatal sensitivity to leaf water potential (δ = -1.2 MPa^{-1}) was selected to best fit excision-rehydration kinetics. This fit was later used for modelling rehydration kinetics. Other parameter values for the fit were: g_{min} = 0.005 mol m^{-2} s^{-1}, α = 0.242 mol m^{-2} s^{-1}, β = -0.00064 g ng^{-1}.

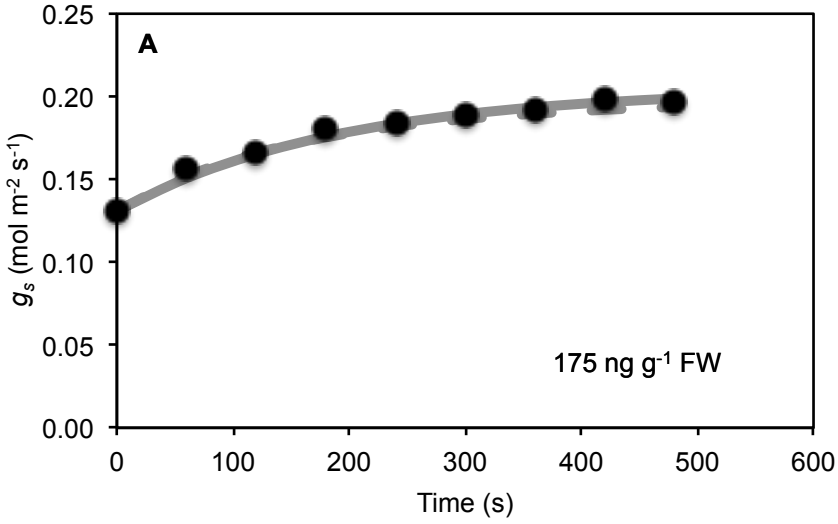
A
175 ng g-1 FW
gs (mol m-2 s-1)
Time (s)
0.25
0.20
0.15
0.10
0.05
0.00
0
100
200
300
400
500
600

438

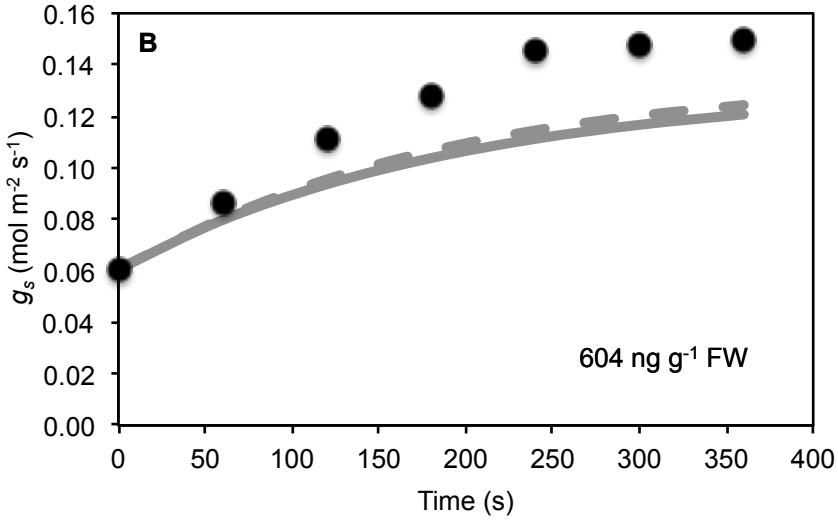
B
604 ng g-1 FW
gs (mol m-2 s-1)
Time (s)
0.16
0.14
0.12
0.10
0.08
0.06
0.04
0.02
0.00
0
50
100
150
200
250
300
350
400

439

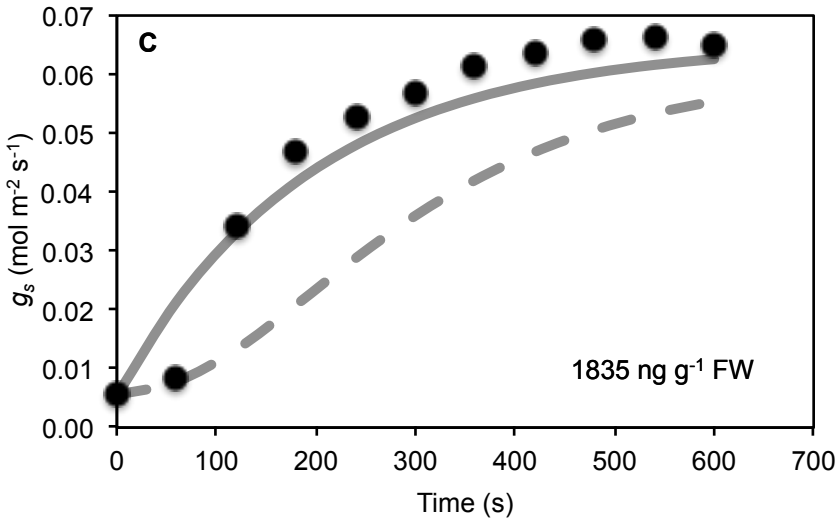
C
1835 ng g-1 FW
gs (mol m-2 s-1)
Time (s)
0.07
0.06
0.05
0.04
0.03
0.02
0.01
0.00
0
100
200
300
400
500
600
700

440

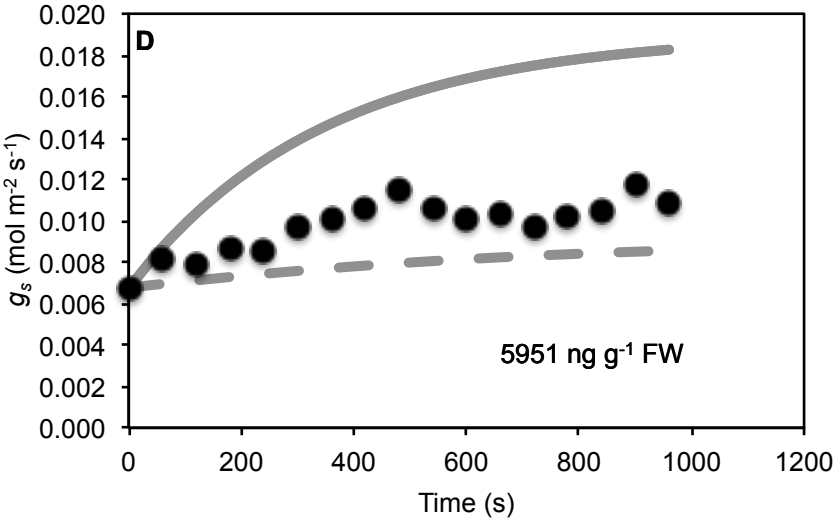

441

442 **Supplemental Figure S4.** Stomatal conductance recovery upon recutting underwater, following
443 drought to increase leaf ABA levels, with modelled recovery using the ABA hydraulic model (solid
444 grey line) and the Tardieu and Davies model (grey dashed line).

445

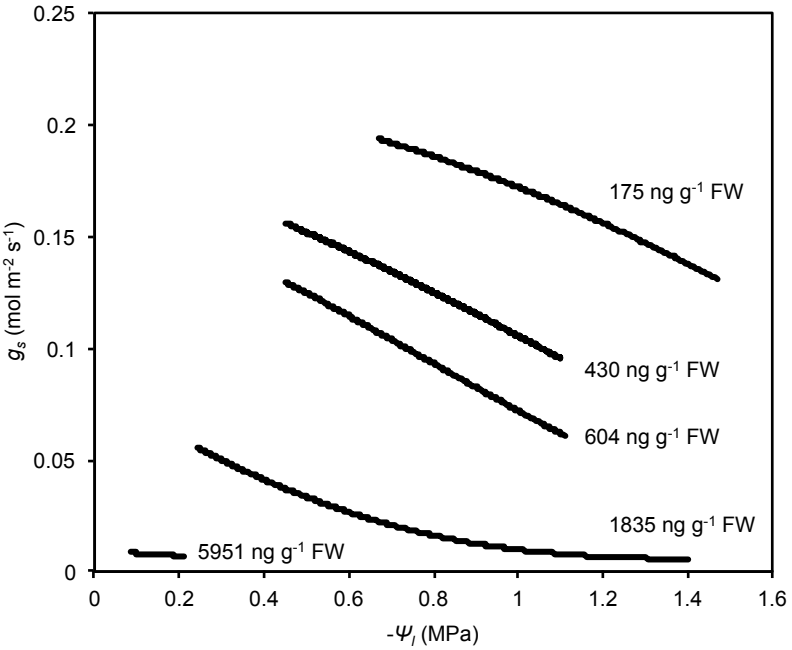

446

447 **Supplemental Figure S5.** Plotted dependence of stomatal conductance on leaf water potential for the
448 Tardieu and Davies model with δ = -1.2 MPa^{-1}, during the simulated excision-rehydration and
449 rehydration following drought kinetics at different ABA levels. Within a simulated dynamic using the
450 Tadieu and Davies model, [ABA] tended to change by a relatively small amount, while simulated Ψ_l
451 changed substantially. The Tardieu and Davies model tended to correspond well with the ABA
452 hydraulic model when the g_s vs. Ψ_l relationship was approximately linear with the same slope as used

in the ABA hydraulic model (i.e. 175 ng g^{-1}, 430 ng g^{-1} and 604 ng g^{-1} cases). Fitting the simulated g_s vs. Ψ_l relationship from the Tardieu and Davies model with a linear line of best fit gave: 175 ng g^{-1}: χ = 0.0755 mol m^{-2} s^{-1} MPa^{-1}, R^2 = 0.994; 430 ng g^{-1}: χ = 0.0949 mol m^{-2} s^{-1} MPa^{-1}, R^2 = 0.996; 604 ng g^{-1}: χ = 0.105 mol m^{-2} s^{-1} MPa^{-1}, R^2 = 0.999; 1835 ng g^{-1}: χ = 0.0503 mol m^{-2} s^{-1} MPa^{-1}, R^2 = 0.928; 5951 ng g^{-1}: χ = 0.0144 mol m^{-2} s^{-1} MPa^{-1}, R^2 = 0.995.